Site-selective spectroscopy of defect chemistry in $SrTiO_3$, Sr_2TiO_4, and $Sr_3Ti_2O_7$

Nigel J. Cockroft,* Steven H. Lee,† and John C. Wright
Department of Chemistry, University of Wisconsin at Madison, Madison, Wisconsin 53706
(Received 4 January 1991)

Eu^{3+}-doped $SrTiO_3$, Sr_2TiO_4, $Sr_3Ti_2O_7$, and $Sr_4Ti_3O_{10}$ phases have been studied by site-selective laser spectroscopy. The spectra of the dominant sites have been identified and assigned to Eu^{3+} substitution on Sr sites with distant charge compensation. The spectra of nonstoichiometric samples show that the nonstoichiometry is accommodated by formation of Ruddlesden-Popper phases. There is no evidence that appreciable numbers of point defects accompany the nonstoichiometry. Additional centers are observed when the dopant concentration is raised. These centers are assigned to locally compensated Eu^{3+} sites and/or clusters of several Eu dopants where point defects provide local compensation.

INTRODUCTION

Perovskites have become a very important class of materials because their ferroelectric, piezoelectric, superconducting, photoconducting, and photochromic properties make them attractive for modern technological applications.[1,2] Small deviations in stoichiometry, purity, oxygen fugacity, and grain structure often affect the defect chemistry underlying the bulk properties.[1] $SrTiO_3$ and $BaTiO_3$ can be insulators or *n*- or *p*-type semiconductors depending on the dopants.[3] It is therefore important to understand the defect chemistry of the perovskites from a fundamental point of view.

Perovksites differ from many materials by resisting the formation of point defects when they become nonstoichiometric.[4] Instead, they form Ruddlesden-Popper phases having different numbers of perovskite layers alternating with layers having a different structure.[4-6] $SiTiO_3$ and its related phases is one of the best-known perovskites. These phases have the general formula $Sr_{n+1}Ti_nO_{3n+1}$, where $n=1,2,\ldots,\infty$ and SrO layers are sandwiched between n perovskite layers. The defects in these ternary compounds depend on the oxygen fugacity, since they can accommodate variable amounts of oxygen.[1] The intrinsic point defects are commonly thought to be oxygen and strontium vacancies [$V_{\ddot{O}}$ and V''_{Sr} (Ref. 7)] at high $p(O_2)$ and V''_O and trivalent Ti (Ti'_{Ti}) at low $p(O_2)$, although other mechanisms remain possible.[8-22] If a trivalent lanthanide such as Eu^{3+} is substituted for Sr^{2+} at high $p(O_2)$ concentrations, two $Eu^{\cdot}_{Sr}$ ions could be compensated by a V''_{Sr} that is distant or there could be local pairing with one $Eu^{\cdot}_{Sr}$. A dimer structure may also form where two $Eu^{\cdot}_{Sr}$ ions are paired with the V''_{Sr}. Another possibility suggested by calculations is Sr''_{Ti} compensation, which is predicted for a SrO excess $SrTiO_3$.[6] There is also evidence that self-compensation could occur with Eu'_{Ti} providing compensation for $Eu^{\cdot}_{Sr}$.[13] The actual compensation mechanism will determine the properties for applications where rare-earth-doped $SrTiO_3$ is used such as positive-temperature coefficient resistors in many refrigerators and color television receivers.

The current understanding of perovskite defect chemistry has been largely inferred from electrical conductivity measurements by Smythe and co-workers[8-11] and Eror and co-workers[12-17] on pure and doped $SrTiO_3$ with different [Sr]/[Ti] ratios. Additionally thermogravimetric analysis,[18,19] x-ray diffraction,[5] and electron microscopy[4] have also provided valuable information. These experiments do not provide information about the microscopic defect chemistry.

Site-selective laser spectroscopy has proved to be a valuable tool for understanding the solid-state chemistry of a material at an atomic level.[23] The crystal-field splittings in the optical absorption and fluorescence spectra of lanthanide-ion dopants reflect the local lanthanide environment. The spectra have excellent sensitivity to the presence of different phases and different local compensations of the lanthanide. The selectivity of the methods make it possible to work with highly defective materials, while the sensitivity and dynamic range make it possible to quantify defect center concentrations over six orders of magnitude. A variety of techniques has been developed that permits a detailed and complete understanding of solid-state defect equilibria.[23,24] The wealth of possible defect equilibria in the perovskites makes it very attractive to use site-selective spectroscopy as a method of sorting out the defect behavior of these important materials.

In this work, we report that site-selective spectroscopy of Eu^{3+} doped in the important $Sr_{n+1}Ti_nO_{3n+1}$ phases. Definitive results are shown for $SrTiO_3$, Sr_2TiO_4, $Sr_3Ti_2O_7$, and attempts to prepare higher $Sr_{n+1}Ti_nO_{3n+1}$ phases are reported. The spectra are very sensitive to the presence of the different phases and are excellent measures of their relative importance. A single dominant Eu center is found in both $SrTiO_3$ and Sr_2TiO_4. Both centers are assigned to nonlocal charge compensation where the Eu occupies the normal Sr lattice site. Two sites are found in $Sr_3Ti_2O_7$ and are assigned to nonlocal compensation where the Eu ions occupy two inequivalent Sr sites. Additional centers are found when the dopant concentration is raised that are attributed to locally compensated Eu sites and/or clusters of several Eu ions and their charge compensations. These same centers are found in doubly doped samples where La^{3+} or Ce^{3+} was added in addition to the Eu^{3+}. In materials that were purposely

prepared to depart from [Sr]/[Ti] stoichiometry, the site-selective spectra show that the nonstoichiometry is accommodated by the formation of appropriate amounts of two Ruddlesden-Popper phases, and there is no evidence that substantial numbers of vacancies or Sr''_{Ti} defects are created by the nonstoichiometry.

THEORY

If the rare-earth charge compensation in the perovskites is accomplished by Sr vacancies (V''_{Sr}) and electrons on Ti sites (Ti'_{Ti}), the relative importance of the locally and distantly compensated rare earths is described by the mass action relationships:[3]

$$K_p=\frac{[(Eu_{Sr}\cdot V_{Sr})']}{[Eu_{Sr}^{\cdot}][V''_{Sr}]}\ , \tag{1}$$

$$K_d=\frac{[(2Eu_{Sr}\cdot V_{Sr})^{\times}]}{[Eu_{Sr}^{\cdot}]^2[V''_{Sr}]}\ , \tag{2}$$

$$K_e=\frac{[(Eu_{Sr}\cdot Ti_{Ti})^{\times}]}{[Eu_{Sr}^{\cdot}][Ti'_{Ti}]}\ . \tag{3}$$

Together with the condition for charge neutrality,

$$2[V_O^{\cdot\cdot}]+[Eu_{Sr}^{\cdot}]=2[V''_{Sr}]+[Ti'_{Ti}]+[(Eu_{Sr}\cdot V_{Sr})']\ , \tag{4}$$

and site and mass conservation relations, these relationships control the relative distribution of sites. The experiments reported in this paper are performed on samples prepared at ambient oxygen pressures so the electronic compensation should not be important relative to V''_{Sr} compensation. If the dopant concentration is low enough to prevent local compensation and dopant clustering but not low enough to make $[V_O^{\cdot\cdot}]$ important, then $[Eu_{Sr}^{\cdot}]$ will be approximately equal to the dopant concentration and $[V''_{Sr}]=[Eu_{Sr}^{\cdot}]/2$. Under these conditions, $[(Eu_{Sr}\cdot V_{Sr})']$ will vary as the square of the dopant concentration [see Eq. (1)] and $[(2Eu_{Sr}\cdot V_{Sr})^{\times}]$ will vary as the cube of the dopant concentration [see Eq. (2)]. Previous workers have often found that $[V''_{Sr}]$ is controlled by external impurity ions and is approximately constant.[3,25] Then $[(Eu_{Sr}\cdot V_{Sr})']$ and $[(2Eu_{Sr}\cdot V_{Sr})^{\times}]$ will vary linearly and quadratically, respectively, with the dopant concentration. The functionalities become more complex at dopant concentrations where local compensation becomes important.

EXPERIMENT

A N_2 laser excited dye laser is used to excite polycrystalline samples that are mounted on a copper holder inside the vacuum jacket of a cryogenic refrigerator at approximately 10 K. Site-selective fluorescence is measured with a 1-m monochromator. The system is interfaced to a small laboratory computer to control the data acquisition and provide simple data analysis. Single-site excitation spectra are obtained by monitoring a fluorescence line while scanning the dye laser. Single-site fluorescence spectra are obtained by exciting a single absorption line and scanning the monochromator. Nonselective excitation spectra are obtained by monitoring all fluorescence transitions with a $\frac{1}{4}$-m monochromator while scanning the dye laser over the absorption lines. A mechanical chopper is used to block laser scatter during the excitation but pass the fluorescence that occurs later when measuring transitions at or near the laser wavelength.

The samples were prepared by a standard method.[11,26] An ethylene glycol/citric acid solution with titanium tetraisopropoxide is combined with appropriate amounts of the rare-earth solution and $SrCO_3$ powder and thermally polymerized. The sample was pressed into a pellet and heated at 800–900 °C for 3 h under ambient pressure to form the phases by sintering. The pellet was removed, ground, and heated to 1420–1450 °C for 16 h to complete the formation of the desired phase and annealing of the crystal lattice. The sample was reground before packing into the copper sample holder to minimize any potential effects from examining only the surface that was in contact with the furnace atmosphere. The identification of the phases in the sample was performed by powder x-ray diffraction. This procedure gave samples with better than 98% purity for $SrTiO_3$ and $Sr_3Ti_2O_{10}$ and better than 99% purity for Sr_2TiO_4. The samples intended to be $Sr_4Ti_3O_{10}$ and higher phases were predominately the $Sr_3Ti_2O_{10}$ phase with small amounts of $SrTiO_3$.

RESULTS

Nonselective excitation spectra of the Eu^{3+} $^7F_0\rightarrow{}^5D_1$ transition were obtained for samples of $SrTiO_3$, Sr_2TiO_4, $Sr_3Ti_2O_7$, and the intended $Sr_4Ti_3O_{10}$ phases and are shown in Figs. 1 and 2. Figure 1 shows the spectra after the final heating of the sample, while Fig. 2 shows the spectra after the initial heating to 900 °C. The $^7F_0\rightarrow{}^5D_1$ spectrum is a useful transition to study as magnetic dipole transitions are allowed for all centers including those with inversion symmetry. The spectral changes from Figs. 2 to 1 reflect differences in the sample environment as the new phases are formed by the high-temperature sintering process and a narrowing of the spectral features as the local environment develops increased order. The figures also indicate the line positions of different sites that are identified by site-selective spectroscopy. Each distinct Eu^{3+} site spectrum can be unambiguously assigned to a particular structural phase by correlating the spectrum with the x-ray diffraction phase determination. The sites are labeled by letters with a subscript that indicates the number of Sr ions in the phase's formula.

The site-selective spectra of the most important fluorescence transitions from both the $^5D_0$ and $^5D_1$ level of the sites in each of the $SrTiO_3$, Sr_2TiO_4, and $Sr_3Ti_2O_7$ phases are shown in Figs. 3–6, respectively. The site-selective spectra for the b_3 site are much weaker than the other sites, and many transitions cannot be measured. The lifetimes of the $^5D_0$ and $^5D_1$ levels are given in Table I. Assignments of energy states are given in Tables II–V for each site using the excitation spectra for the $^5D_1$ and

TABLE I. $^5D_0$ level lifetimes in μsec.

Site	Lifetime
a_1	1160
a_2	540
d_2, e_2	338
a_3	350
b_3	1700
a_4	1200

$^5D_0$ levels and the fluorescence spectra of the $^5D_0$ and $^5D_1$ levels for the ^7F_J levels. Note the weak zero phonon line of the a_1 site in the $^5D_0 \rightarrow {}^7F_0$ transition (see Fig. 3) compared with the phonon sideband. This is characteristic of sites with near-cubic symmetry. There is a temperature-dependent and perhaps also a sample-dependent shift in the energy levels of the a_1 site because of the phase transition from cubic to orthorhombic sym-

TABLE II. Energy levels of a_1 site (cm^{-1} in air).

Level	Measured from fluorescence $^5D_0$ (cm^{-1})	$^5D_1$ (cm^{-1})
$^7F_1$	329.5	329.1
$^7F_2$		963.5
	1 003.7	1 003.9
	1 033.8	1 034.0
$^7F_3$		1 811.5
		1 828.8
		1 903.4
		1 926.6
		1 986.4
$^7F_4$	2 578.2	
	2 628.5	
	2 764.5	
	3 004.7	
	3 020.7	
	3 081.2	
$^5D_0$	17 252.8	
$^5D_1$	19 006.5	
	19 022.0	

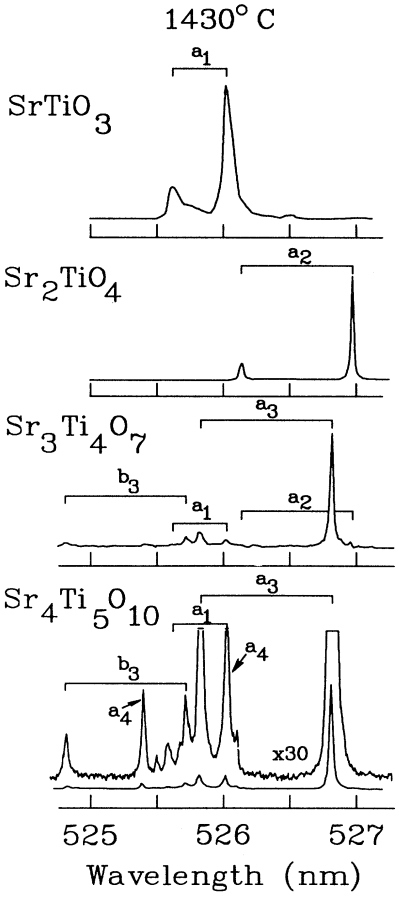

FIG. 1. Excitation spectra of $^7F_0 \rightarrow {}^5D_1$ transition with broadband fluorescence monitoring for each of the important $Sr_{n+1}Ti_nO_{3n+1}$ phases prepared at 1430 °C. The lines associated with the important Eu^{3+} sites are indicated.

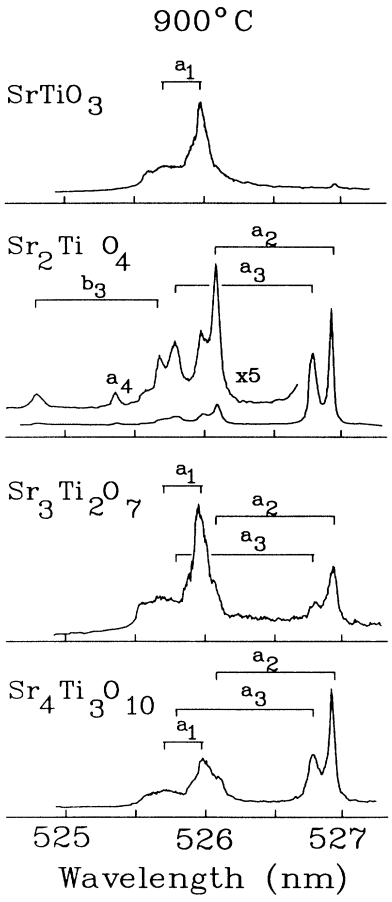

FIG. 2. Excitation spectra of $^7F_0 \rightarrow {}^5D_1$ transition with broad band fluorescence monitoring for each of the phases shown in Fig. 1 but prepared at 900 °C.

TABLE III. Energy levels of a_2 site (cm^{-1} in air).

Level	$^5D_0$	$^5D_1$
$^7F_1$	310	
	447	
$^7F_2$		892
	1 014	1 015
	1 104	1 109
$^7F_3$	1 835	1 839
		1 898
		1 926
$^7F_4$		2 800
	2 842	2 841
	2 967	2 973
$^5D_0$	17 230.1	
$^5D_1$	18 978	
	19 008	

TABLE IV. Energy levels for e_2 site (cm^{-1} in air).

Level	$^5D_0$	$^5D_1$
$^7F_1$	238	
$^7F_2$	813	
	864	866
	928	
	1 334	
	1 348	1 350
	1 365	1 367
$^7F_3$		1 977
	2 055	
	2 090	2 089
	2 112	2 116
	2 188,2 193	2 193
	2 262	
$^7F_4$	2 924	2 926
	2 967	
	2 990	2 993
	3 020	3 024
$^5D_0$	17 310	
$^5D_1$	19 026	

metry at 105 K.[27] The details of the a_1 site's temperature dependence in a single crystal will be reported elsewhere.[28] The level positions listed in Table II reflect the limiting values at low temperatures. They agree with values obtained in single-crystal work, but the line widths of the a_1 transitions in these sintered powders are larger than the single crystals and the line shapes are asymmetric. The increased linewidth and asymmetry are tentatively attributed to variations in the temperature of polycrystallline components of the $SrTiO_3$ powder packed in the sample holder. The sample temperature is dependent on interplay from the backside cooling of the refri-

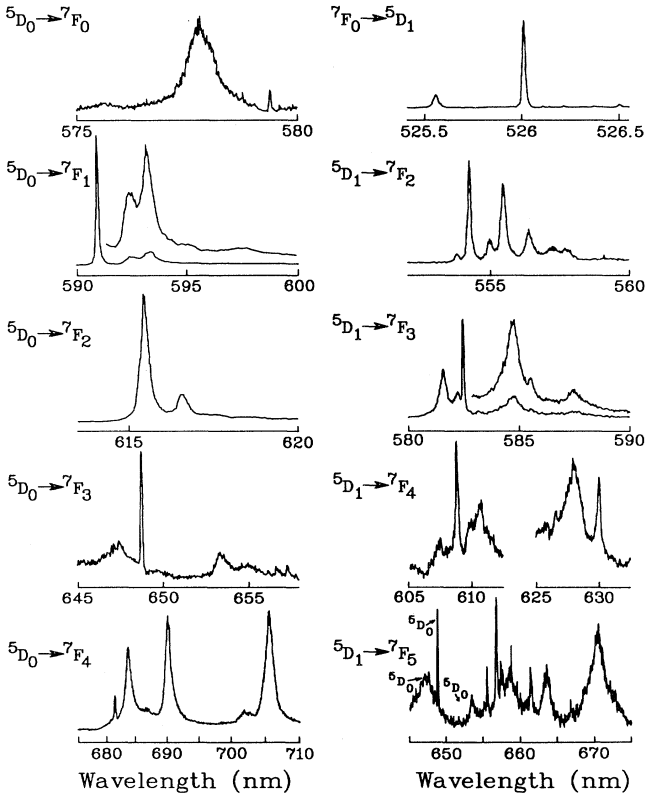

FIG. 3. Site-selective spectra for the important transitions of the a_1 site in $SrTiO_3$. Lines from other fluorescing manifolds are indicated.

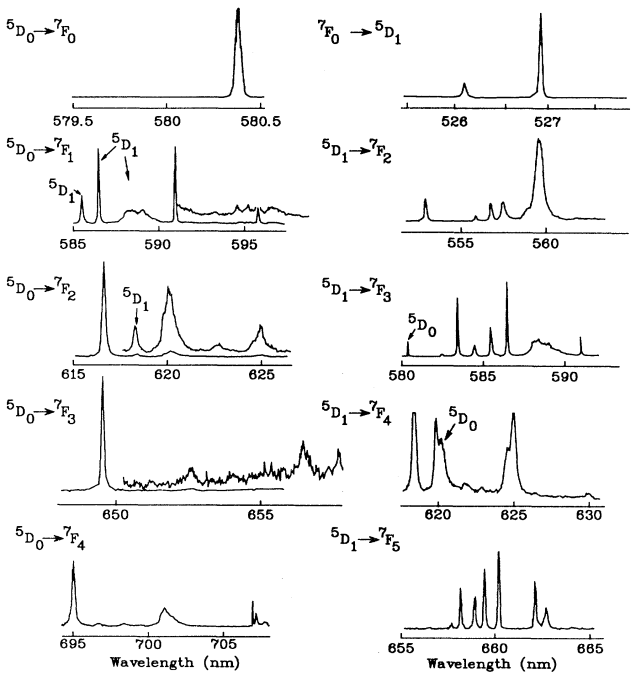

FIG. 4. Site-selective spectra for the important transitions of the a_2 site in Sr_2TiO_4. Lines from other fluorescing manifolds are indicated.

TABLE V. Energy levels for the a_3 site (cm^{-1} in air).

Level	$^5D_0$	$^5D_1$
$^7F_1$	302	
$^7F_2$		902
		1 019
	1 051	1 054
	1 108	1 109
	1 125	1 126
	1 149	
	1 182	
$^7F_3$	1 830	1 831
		1 913
		1 921
		1 958
	1 983	1 980
$^7F_4$	2 800	
	2 949	2 951
		2 997
	3 090	
$^5D_0$	17 236	
$^5D_1$	18 982	
	19 018	

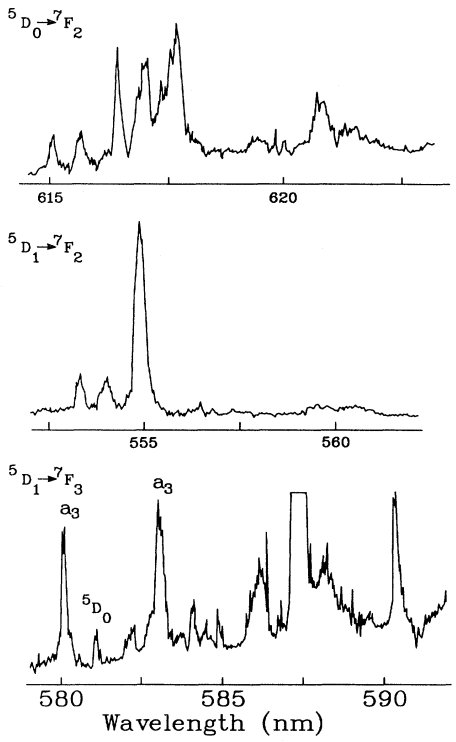

FIG. 6. Site-selective spectra for the important transitions of the b_3 site in $Sr_3Ti_2O_7$. Lines from other sites that spectrally overlap with b_3 lines are indicated, as are lines from other fluorescing manifolds.

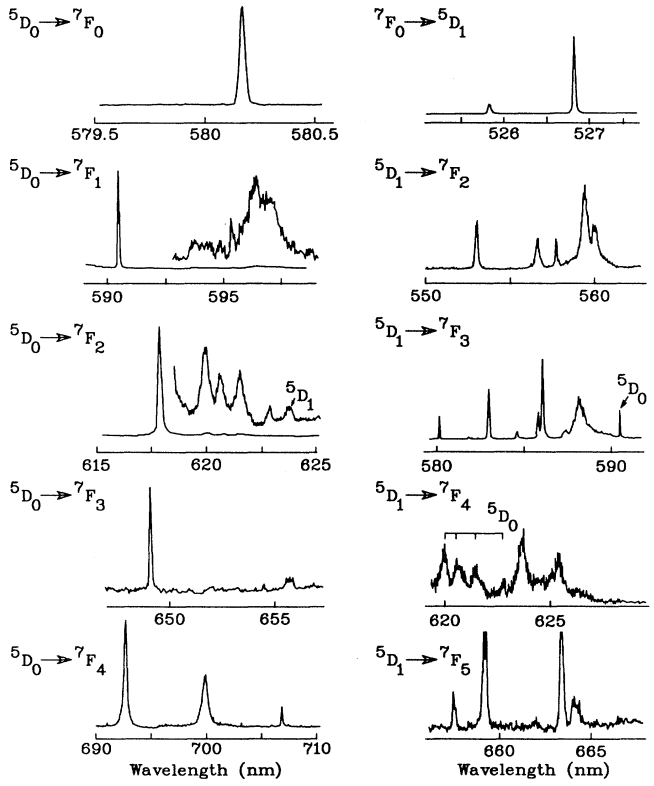

FIG. 5. Site-selective spectra for the important transitions of the a_3 site in $Sr_3Ti_2O_7$. Lines from other fluorescing manifolds are indicated.

gerator and copper sample block and the black body radiation from the room. The temperature of individual crystallites will depend on its crystallinity, its thermal contact with surrounding particles, and its exposure to the room radiation. Since the $SrTiO_3$ phase transition results in increased splitting between the two $^5D_1$ energy levels from 0 cm^{-1} at 105 K to 15.5 cm^{-1} at 10 K, the observed spectrum will be an average of the contributions from all particles in the sample. The coldest particles will have the widest splittings and will contribute to the outermost peaks. The warmest will have the smallest splittings and will contribute to the intensity between the peaks. Heating a $SrTiO_3$ sample at 1050 °C for 52 h reduced the linewidths by 30–40 %. This reduction is consistent with the expected formation of larger crystals resulting in fewer surface-surface contact points. Sites of other phases did not exhibit broadened transitions, since they do not have temperature-dependent line positions.

In the $SrTiO_3$ sample of Fig. 1, the two strong transitions come from the site labeled a_1. The much weaker structure in the spectra for this phase will be discussed in detail elsewhere and compared to minority centers in single crystals. The two transitions observed in the Sr_2TiO_4 phase in Fig. 1 are from the site labeled a_2. The two intense lines from the $Sr_3Ti_2O_7$ phase in Fig. 1 are associated with the site labeled a_3, while the weaker lines are associated with the site labeled b_3. There are also weak

lines from the a_1 and a_2 sites of $SrTiO_3$ and Sr_2TiO_4 phases in the $Sr_3Ti_2O_7$ sample. Any of the more minor sites are much weaker and are not visible in the spectra as plotted. Note the strong similarity of the line positions and relative intensities between the a_2 and a_3 site spectra and the difference they have from those of the a_1 site. There are two lines in the $Sr_4Ti_3O_{10}$ phase spectrum that site-selective spectroscopy shows correspond to the same site labeled a_4 because it is believed to correspond to the $Sr_4Ti_3O_{10}$ phase. The spectrum is dominated by lines from the $Sr_3Ti_2O_7$ and $SrTiO_3$ phases, in agreement with the x-ray diffraction results. Previous attempts have also failed to produce single-phase $Sr_4Ti_3O_{10}$.[5]

The branching ratios for the b_3 site fluorescence transitions are quite different from the a_3 site found in the same phase. For the b_3 site, the relative intensities of the $^5D_0 \rightarrow {}^7F_{0,1,2}$ transitions are in the ratio of 1:98:3, while the ratios are 1:1:5 for the a_3 site. The dominance of the $^5D_0 \rightarrow {}^7F_1$ transition is often found for near cubic-symmetry sites where electric dipole transitions are weak and the magnetic dipole transitions with $\Delta J = \pm 1$ dominate. This is also reflected in the relative intensities of the $^5D_1 \rightarrow {}^7F_{2,3}$ transitions that have the ratio 40:1 for the b_3 site and 7.5:1 for the a_3 site. It is believed that the near cubic symmetry of the b_3 site causes the weak transitions for $\Delta J \neq \pm 1$. The long $^5D_0$ lifetime for b_3 (Table I) also indicates a near cubic symmetry.

Small deviations from exact stoichiometry of any phase would be expected to increase the concentrations of defects such as V''_{Sr} for [Sr]/[Ti] ratios smaller than stoichiometric and $V_{\ddot{O}}$ (or perhaps Sr''_{Ti}) for [Sr]/[Ti] ratios larger than stoichiometric. These changes would have important effects on the relative site distribution of aliovalent ions such as Eu^{3+}. The deviations would also lead to the formation of other phases. Figure 7 shows the changes in the spectra for a series of [Sr]/[Ti] ratios deviating from the Sr_2TiO_4 phase. No new sites appear in the spectra, but there are changes in the relative concentrations of different phases. For [Sr]/[Ti]=1.89, the major a_3 line appears with an intensity of approximately 11% of the a_2 transition. This ratio is close to the 14% value expected if the sites have the same transition probability. Similarly, when [Sr]/[Ti]=1.51, the a_2 site intensity is only approximately 6.6% of the a_3 transition. Again, this value is quite close to the 4.1% value expected. If the [Sr]/[Ti]=2.09, there is no change in the spectrum nor are any other $Sr_{n+1}Ti_nO_{3n+1}$ phases expected for this value.

If the dopant concentration in stoichiometric Sr_2TiO_4 is raised, new sites appear in the spectrum that are not associated with the dominant centers of any of the identifiable phases. The nonselective excitation spectra of the $^7F_0 \rightarrow {}^5D_1$ transition are shown in Fig. 8. The intensity of these sites increases very rapidly over the dopant concentration range from 0.05 to 0.2 mol % and then appears to remain relatively constant. The lines labeled c_2, d_2, e_2, f_2, g_2, and h_2 are located at 525.39, 525.57, 525.61, 525.74, 525.85, and 526.37 nm, respectively. The d_2 and e_2 lines at 525.6 nm are not resolved in many of the samples. Site-selective spectroscopy shows that all of the new lines correspond to individual sites, including the two closely spaced lines at 525.6 nm. The site-selective spectra for the sites are shown in Fig. 9. Detailed energy levels for the e_2 site are given in Table IV, since it is generally the most intense in the series. Site-selective excita-

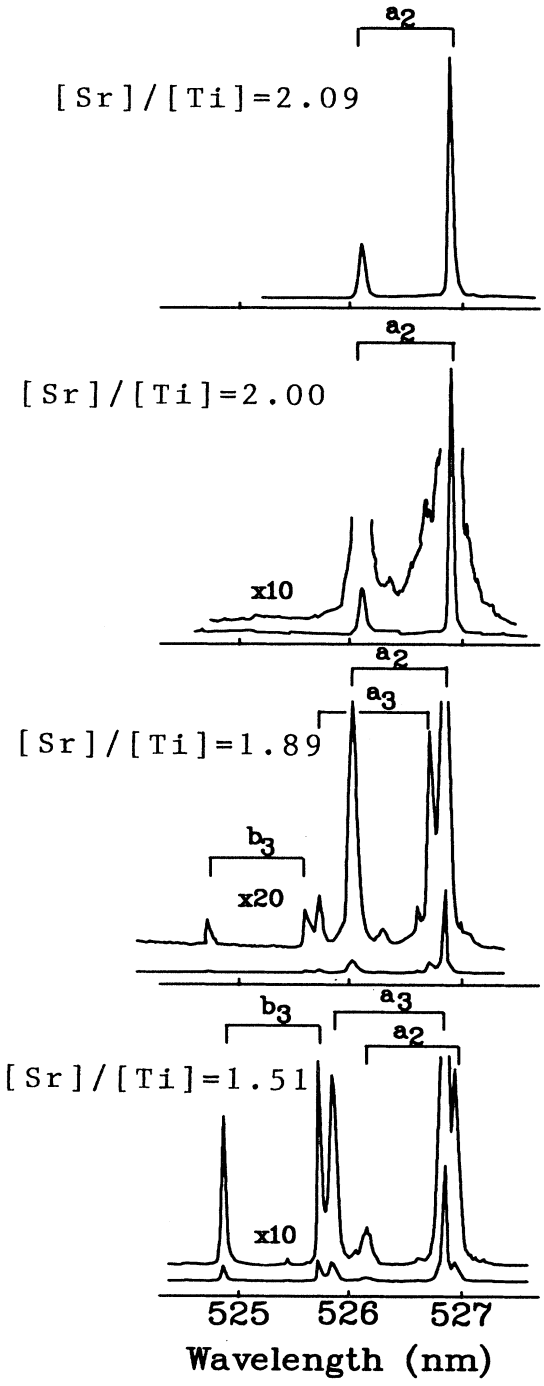

FIG. 7. The excitation spectra of the $^7F_0 \rightarrow {}^5D_1$ transition with broadband fluorescence monitoring for samples with different [Sr]/[Ti] ratios. The lines from the different Eu^{3+} sites are indicated.

tion spectroscopy was used to determine that the e_2 site $^5D_1$ excitation transition intensity was 1850 times greater for 0.2% Eu^{3+} concentration than for 0.02% Eu^{3+}. These new transitions are clearly different from those identified for the other phases indicating that these new centers cannot be attributed to the formation of the other phases. Instead, they are attributed to new defect centers that are forming within the Sr_2TiO_4 phase because of the raised Eu^{3+} concentration.

In order to identify whether any of these sites are associated with clusters of dopant ions, double-doping experiments were performed. La^{3+} or Ce^{3+} were added as codopants to Eu^{3+}-doped samples, since neither interferes with the Eu^{3+} spectroscopy. If there are rare-earth-ion cluster sites, one would expect that Eu^{3+} ions would substitute into clusters that were primarily La^{3+} or Ce^{3+}. Since these ions have appreciably different ionic radii, the Eu^{3+} crystal-field splitting would change and new sites would appear that were similar to but distinct from the pure Eu^{3+} cluster sites. The presence of codopant ions can also affect the Eu^{3+} indirectly by raising the total concentration of defects requiring charge compensation so the relative number of distantly and locally compensated Eu sites may change.

Figure 10 shows the spectra of samples ranging from

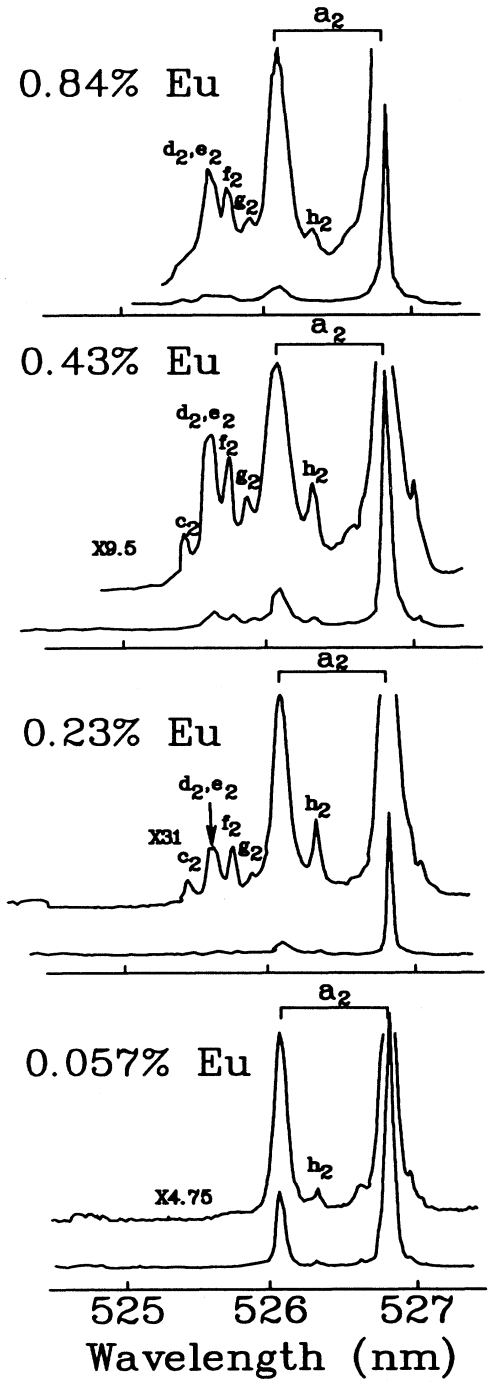

FIG. 8. The excitation spectra of the $^7F_0 \rightarrow {}^5D_1$ transition with broadband fluorescence monitoring for samples with different Eu concentrations. The lines from the different Eu^{3+} sites are indicated.

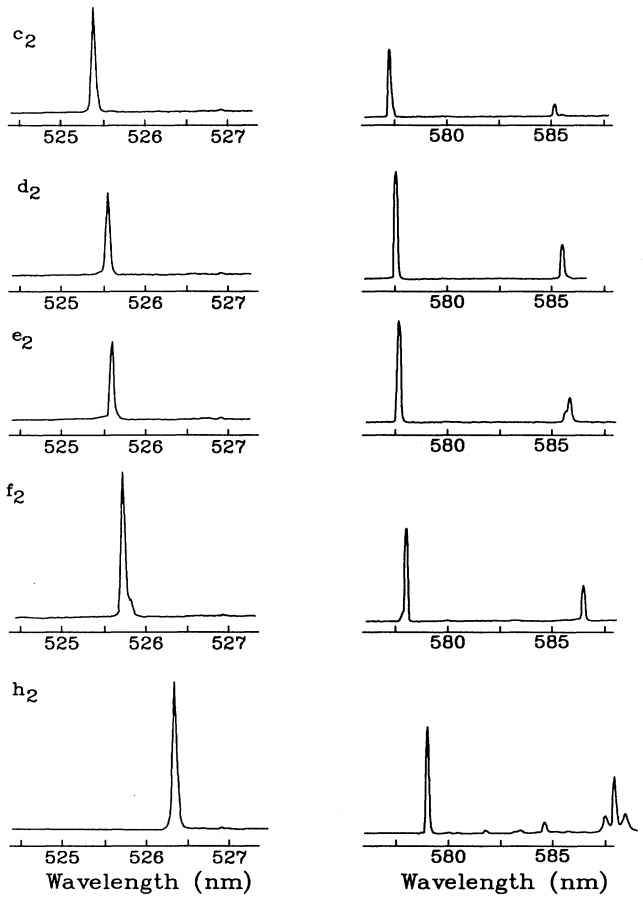

FIG. 9. Single-site spectra of the $^7F_0 \rightarrow {}^5D_1$ transition (left-hand column) and the $^5D_0 \rightarrow {}^7F_{0,1}$ transitions of the c_2, d_2, e_2, f_2, and h_2 sites in Sr_2TiO_4.

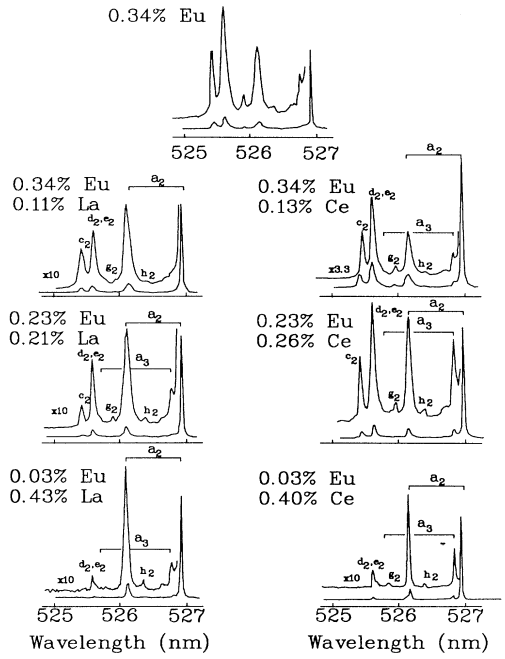

FIG. 10. The excitation spectra of the $^7F_0 \rightarrow {}^5D_1$ transition with broadband fluorescence monitoring for doubly doped samples with the indicated concentrations. The lines from the different Eu^{3+} sites are indicated.

high codopant concentrations and low Eu concentrations to low codopant concentrations and high Eu concentrations. The total rare-earth concentration was kept constant. The behavior of the site distribution is very similar for the two codopants. The new sites, c_2 through h_2, appear for both the La and Ce codopants. No additional Eu^{3+} transitions are observed. It is interesting that both samples with the highest codopant concentrations produce only the sites labeled d_2 and e_2. The other new sites do not appear until the Eu concentration is raised.

There are apparently sources of irreproducibility associated with the sample preparation at higher concentration. The intensity of the a_2 site lines does not scale directly with the nominal dopant concentrations indicating that there may be irreproducibility in the amount of Eu^{3+} that actually enters the Sr_2TiO_4 lattice. Some samples that should have had concentrations sufficient to produce the new sites did not. If those samples are resintered, the sites are observed but with less than the intensity expected from experience with other samples. These problems are attributed to differences in the actual trivalent dopant concentration entering the lattice and to trace impurities that have been introduced in the sintering process by the crucibles and the furnace. The samples did exhibit the characteristic fluorescence of Eu^{2+} and Eu^{3+} with different samples showing different relative amounts of the two valence states. The relative amounts did not correlate with the differences in the spectra though. It is observed that the irreproducibilities are not important for samples prepared together as was done for the samples used for Figs. 7, 8, and 10.

In order to determine whether the sites might be associated with common impurities occupying Ti sites, two samples were prepared with 0.055% Eu, 0.03% Na, and 0.055% Eu, 0.03% Cr. The spectra in both cases were identical to the low-concentration Sr_2TiO_4 phase, and there were no indications of new lines that would be associated with the impurities added. Of course, there are many other impurities that could be present at low concentration.

DISCUSSION

The spectra of the Eu^{3+} ion center provide an indication of the local environment. For example, the $^5D_1$ manifold comprises one level for a cubic symmetry center, two levels for some high-symmetry centers, and three levels for low-symmetry centers. Centers of cubic symmetry will have very weak transitions except for the magnetic dipole allowed $\Delta J = \pm 1$ transitions.

The spectrum of Eu^{3+}:$SrTiO_3$ was previously studied by Weber and Schaufele.[29,30] They reported a single center and attributed it to the distantly compensated $Eu_{Sr}^{\cdot}$ site with cubic symmetry. $SrTiO_3$ actually has a phase transition from cubic to orthorhombic symmetry at 105 K.[27] Although Weber and Schaufele did not resolve the small $^5D_1$ splitting with their 77-K measurements, we have confirmed that their site is our a_1 site. At our lower temperatures, the $^5D_1$ levels are very well resolved. Spectra recorded above 105 K unambiguously confirm the a_1 site is the isolated $Eu_{Sr}^{\cdot}$ center.

It is interesting to note that the b_3 site of $Sr_3Ti_2O_7$ has relative intensities for the $^5D_J \rightarrow {}^7F_J$ transitions and $^5D_0$ level lifetimes that are very similar to the a_1 site of $SrTiO_3$, while the a_3 site has crystal-field splittings, relative intensities, and level lifetimes that are very similar to the a_2 site of Sr_2TiO_4. In $Sr_3Ti_2O_7$, the Sr sites in the perovskite layers have a similar local environment to the Sr site in $SrTiO_3$ while the Sr sites in the SrO layers have a similar environment to the Sr site in Sr_2TiO_4. There are twice as many Sr sites in the SrO layers of $Sr_3Ti_2O_7$ as the perovskitelike layers, so assuming equal transition strengths, there would be a difference of two in the relative intensities observed for the corresponding Eu^{3+} substituted sites. This suggests the similarity of the b_3 and a_3 sites to the corresponding $SrTiO_3$ a_1 and Sr_2TiO_4 a_2 site spectra and lifetimes arise because the b_3 site is associated with the perovskite layers, while the a_3 site corresponds to SrO layer substitution, although this evidence is not definitive.

The experiments on samples with different stoichiometric ratios [Sr]/[Ti] show that the only effect on the local environment of Eu ions is a change in the relative amounts of the different possible phases. The changes are equal to what one expects for each [Sr]/[Ti] ratio. If excess SrO or TiO_2 is actually creating additional $V_O^{\cdot\cdot}$, $V_{Ti}^{''''}$ or $V_{Sr}^{\cdot\cdot}$ defects in one of the phases, there is no evidence from the spectra that they are involved in

pairing equilibria with the $Eu_{Sr}^{\cdot}$. We interpret the spectra as additional evidence that these phases resist defect formation by readily forming the different Ruddlesden-Popper layered phases.

The presence of aliovalent probe ions must introduce defects to provide charge compensation, and it is interesting to see that new sites become significant in Sr_2TiO_4 when the dopant concentrations reach levels of approximately 0.1 mol % or higher. One expects a strong concentration dependence for the formation of $(Eu_{Sr}\cdot V_{Sr})'$ from the simple mass action considerations described in the theory section. It should have a quadratic concentration dependence during its initial appearance. The experiments with the codopant ions show that the same new Eu^{3+} sites can be formed by adding high concentrations of the La^{3+} or Ce^{3+} ions. If the Eu^{3+} concentration is low, only the d_2,e_2 sites appear although they are not as dominant as in samples where Eu^{3+}-ion concentration is high. At higher Eu^{3+} concentrations, the d_2,e_2 sites become more important and the c_2, f_2, h_2, and g_2 sites also appear. There are several possible interpretations. The d_2,e_2 sites may correspond to a locally compensated $(Eu_{Sr}\cdot V_{Sr})'$ center. It forms when the codopant raises the $[V_{Sr}'']$ concentration and therefore promotes the formation of the $(Eu_{Sr}\cdot V_{Sr})'$ center according to Eq. (1). The weaker intensity of the d_2,e_2 sites in the codoped samples may result because the pairing constant, K_p, is larger and there is more local compensation for La or Ce dopants than Eu. As the Eu concentration is raised, the $[V_{Sr}'']$ concentration is raised relative to the codoped samples so there is more pairing with the Eu to increase the d_2,e_2 site intensities. The other centers appear at higher Eu concentrations because they may correspond to clusters that are formed from Eu. Dimers of the type $(2Eu_{Sr}\cdot V_{Sr})^{\times}$, for example, should increase as the cube power of the Eu^{3+} concentration. It is possible that the same centers may not form from the larger La and Ce ions. There are numerous similar examples in the fluorite system where the amount of pairing and clustering varies strongly for different ionic radii rare earths. The possibility of self-compensation can also not be ruled out at this point.

These interpretations are necessarily somewhat speculative, especially considering the uncertainties with the impurities and amount of dopant incorporation. Further progress, including specific assignment of d_2-h_2, structures must await developments that achieve control of these uncertainties.

CONCLUSIONS

The local environment of the $Sr_{n+1}Ti_nO_{3n+1}$ phases can be probed by site-selective spectroscopy of rare-earth-doped materials. Eu^{3+} appears to readily occupy Sr^{2+} sites in any of the phases. If the rare-earth concentration is low, the presence of the dopant does not affect the material, and the rare-earth fluorescence accurately reflects the relative importance of the different phases. The Eu distribution is apparently very uniform and does not strongly prefer specific phases, since the relative intensity from the different phases in sintered mixtures follows the actual phase mixture. The inhomogeneous broadening of Eu^{3+} transitions can also provide an indication of local disorder. The number of rare-earth sites in the spectra matches the number expected for the $SrTiO_3$, Sr_2TiO_4, and $Sr_3Ti_2O_7$ phases. The spectra of materials prepared with different [Sr]/[Ti] ratios reflect the mixture of the Ruddlesden-Popper phases appropriate to the ratio. The selectivity of laser excitation and the relative simplicity of Eu^{3+} spectra provide considerably better sensitivity to strontium impurity phases than conventional power x-ray-diffraction techniques. This technique also provides greater sensitivity to local defect association than any previously reported defect study on these materials. When the rare-earth concentration is raised, new sites appear that are attributed to the introduction of V_{Sr}'' defects by the dopant. The sites correspond to local compensation of single or multiple rare-earth ions.

ACKNOWLEDGMENTS

This research was supported by the National Science Foundation under Grant No. DMR-8815398. Acknowledgment is also made to the Donors of The Petroleum Research Fund, administered by the American Chemical Society for the partial support of this research.

*Present address: Los Alamos National Laboratories, Los Alamos, NM 87545.

†Present address: Department of Chemistry, Walla Walla College, College Place, WA 99324.

[1]Y. H. Han, M. P. Harmer, Y. H. Hu, and D. M. Smyth, in *Transport in Nonstoichiometric Compounds,* edited by George Sinkovich and V. S. Stubican, Vol. 29 of NATO Advanced Study Institute (Plenum, New York, 1985).

[2]J. G. Bednorz and K. A. Muller, Z. Phys. B **64**, 189 (1986).

[3]N. Eror, in *Transport in Nonstoichiometric Compounds* (Ref. 1).

[4]R. J. D. Tilley, J. Solid State Chem. **21**, 293 (1977).

[5]S. N. Ruddlesden and P. Popper, Acta Crystallogr. **11**, 54 (1958).

[6]K. R. Udayakumar and A. N. Cormack, J. Phys. Chem. Solids **50**, 55 (1989).

[7]F. Bridges, G. Davies, J. Robertson, and A. M. Stoneham, J. Phys.: Condens. Matter **2**, 2875 (1990).

[8]N. H. Chan and D. M. Smyth, J. Electrochem. Soc. **123**, 1584 (1976).

[9]D. M. Smyth, J. Solid State Chem. **16**, 73 (1976).

[10]D. M. Smyth, J. Solid State Chem. **20**, 359 (1977).

[11]N. H. Chan, R. K. Sharma, and D. M. Smyth, J. Electrochem. Soc. **128**, 1762 (1981).

[12]U. Balachandran and N. G. Eror, J. Mater. Sci. **17**, 2133 (1981).

[13]N. G. Eror and U. Balachandran, J. Solid State Chem. **40**, 85 (1981).

[14]U. Balachandran and N. G. Eror, J. Solid State Chem. **39**, 351

(1981).
[15]U. Balachandran and N. G. Eror, J. Electrochem. Soc. **129**, 1021 (1982).
[16]N. G. Eror and U. Balachandran, J. Am. Ceram. Soc. **65**, 426 (1982).
[17]B. Odekirk, U. Balachandran, N. G. Eror, and J. S. Blakemore, Commun. Am. Ceram. Soc. **66**, C22 (1983).
[18]B. F. Flandemeyer, A. K. Agarwal, H. U. Anderson, and M. N. Nasrallah, J. Mater. Sci. **19**, 2593 (1984).
[19]B. F. Flandermeyer, M. N. Nasrallah, D. H. Sparlin, and H. U. Anderson, in *Transport in Nonstoichiometric Compounds* (Ref. 1).
[20]H. Yamada and G. R. Miller, J. Solid State Chem. **6**, 169 (1973).
[21]G. M. Choi, H. L. Tuller, and D. Goldschmidt, Phys. Rev. B **34**, 6972 (1986).
[22]G. M. Choi and H. L. Tuller, J. Am. Ceram. Soc. **71**, 201 (1988).
[23]J. C. Wright, Cryst. Lattice Defects Amorph. Matter **12**, 505 (1985).
[24]K. M. Cirillo-Penn and J. C. Wright, Phys. Rev. B **15**, 10 799 (1990).
[25]I. Burn and S. Nierman, J. Mater. Sci. **17**, 3510 (1982).
[26]M. Pechini, U. S. Patent No. 3,330,697 (1967).
[27]K. A. Muller, W. Berlinger, and F. Waldner, Phys. Rev. Lett. **21**, 814 (1968).
[28]N. J. Cockroft and J. C. Wright, Phys. Rev. B (to be published).
[29]M. J. Weber and R. F. Schaufele, Phys. Rev. **138**, A1544 (1965).
[30]M. J. Weber and R. F. Schaufele, J. Chem. Phys. **43**, 1702 (1965).